Muscleblind-like 1 (Mbnl1) Promotes Insulin Receptor Exon 11 Inclusion via Binding to a Downstream Evolutionarily Conserved Intronic Enhancer*□S

Supriya Sen[‡§], **Indrani Talukdar**[‡§], **Ying Liu**[¶], **Joseph Tam**[¶], **Sita Reddy**[‖], and **Nicholas J. G. Webster**[‡§1]

From the ‡Medical Research Service, Veterans Affairs San Diego Healthcare System, San Diego, California, the §Department of Medicine, University of California, San Diego, La Jolla, California 92093-0673, the ¶University of Hong Kong, Hong Kong, China, and the ‖Institute for Genetic Medicine, Keck School of Medicine, University of Southern California, Los Angeles, California 90089

The insulin receptor exists as two isoforms, IR-A and IR-B, which result from alternative splicing of exon 11 in the primary transcript. These two isoforms show a cell-specific distribution, and their relative proportions also vary during development, aging, and in different disease states. We have previously demonstrated that both intron 10 and the alternatively spliced exon 11 contain regulatory sequences that affect insulin receptor splicing both positively and negatively and that these sequences bind the serine/arginine-rich (SR) proteins SRp20 and SF2/ASF and the CELF protein CUG-BP1. In this study, we describe a new intronic splicing element within intron 11 that is highly conserved across species. Using minigenes carrying deletion mutations within intron 11, we demonstrated that this sequence functions as an intronic splicing enhancer. We subsequently used RNA affinity chromatography to identify Mbnl1 as a splicing factor that recognizes this enhancer. By ribonucleoprotein immunoprecipitation, we also established that Mbnl1 binds specifically to the *INSR* (insulin receptor gene) RNA. Overexpression or knockdown of Mbnl1 in hepatoma and embryonic kidney cells altered the levels of exon 11 inclusion. Finally, we showed that deletion of the intronic enhancer eliminates the ability of Mbnl1 to promote exon inclusion. Collectively, these findings demonstrate a role for Mbnl1 in controlling insulin receptor exon 11 inclusion via binding to a downstream intronic enhancer element.

In mammals, alternative splicing is a common strategy for creating functional diversity in proteins to confer cell and developmentally specific functions. Given its important role, it is not surprising that a recent estimate has proposed that 50–60% of mutations linked to disease affect RNA splicing (1, 2). The majority of human genes undergo alternative pre-mRNA splicing through the use of competing 5′ or 3′ splice sites or through alternative inclusion/exclusion of exons in the pre-mRNA. These alternative exons often contain splice sites that diverge from the consensus, and the presence of *cis* regu-latory elements within the exon and/or the flanking introns determines whether these exons are recognized (3–5). These *cis*-elements can either have a positive (enhancer) or negative (silencer) effect on splicing. Both enhancers and silencers are thought to function through binding to specific *trans*-acting protein factors (6). Differences in the expression or activity of these *trans*-acting factors may modulate the recognition of the alternative exon and lead to developmental or tissue-specific differences in splicing. Proteins that bind to specific sequence elements to affect splice site selection include SR proteins, hnRNPs,[2] and other related RNA-binding proteins such as the CELF family, TIA-1, NOVA1, and A2BP1 (also known as Fox-1) (7–13). Adding a further layer of regulation, local context, such as RNA secondary structure, may influence the way that binding motifs are recognized by their cognate factors (14–16).

The human insulin receptor (IR) is encoded by a single *INSR* gene (insulin receptor gene) that is located on chromosome 19 and is composed of 22 exons. Transcription of the gene gives rise to two protein isoforms, however, that differ by a 12-amino acid insertion in the hormone-binding domain of the receptor due to alternative splicing of exon 11. This alternative splicing event is restricted to mammals and is not seen in the chicken or frog genes (17). The IR isoform lacking exon 11 (IR-A) binds both insulin and insulin-like growth factor-II, whereas the exon 11+ isoform (IR-B) only binds insulin (18). In the adult, the IR-B is expressed predominantly in the insulin-sensitive tissues liver, muscle, adipocytes, and kidney (19–21) that regulate glucose homeostasis. IR-A is expressed predominantly in fetal cells and the early embryo, including the trophoblast and inner cell mass of the blastocyst (18, 22), and there is genetic evidence that the insulin receptor may mediate some of the growth-promoting effects of insulin-like growth factor-II on the mouse embryo (23). Inclusion of IR exon 11 is both developmentally and hormonally regulated and is altered in a number of disease states such as type II diabetes, myotonic dystrophy, aging, and cancer (24–29). The dysregulation of the alternative splicing of the IR may therefore have important consequences for insulin and insulin-like growth factor-II sensitivity and responsiveness. This makes the IR gene an attractive model system for studying

---

□S The on-line version of this article (available at http://www.jbc.org) contains supplemental Figs. S1–S4.
[1] To whom correspondence should be addressed: Stein Clinical Research Bldg. 201, Dept. of Medicine, 0673, University of California, San Diego, 9500 Gilman Dr., La Jolla, CA 92093-0673. Tel.: 858-534-6275; Fax: 858-534-6653; E-mail: nwebster@ucsd.edu.

[2] The abbreviations used are: hnRNP, heterogeneous nuclear ribonucleoprotein; IR, insulin receptor; ANOVA, analysis of variance; BisTris, 2-[bis(2-hydroxyethyl)amino]-2-(hydroxymethyl)propane-1,3-diol; nt, nucleotide; RT, reverse transcription; siRNA, small interfering RNA.

the mechanism of alternative splicing, and identification of regulatory sequences and factors that control the IR-B/IR-A ratio is of critical importance for the understanding of the role of IR in different disease states.

Myotonic dystrophy type 1 (DM1), one of the most common forms of muscular dystrophy, is associated with muscle hyperexcitability, muscle wasting, cardiac defects, cataracts, smooth muscle disturbances, and insulin resistance. DM1 is caused by an expansion of CUG repeats in the 3′-untranslated region of the DM protein kinase (*DMPK*) mRNA (30, 31). This expansion sequesters the muscleblind (Mbnl) proteins, causes an increase in the expression of a CUG-binding protein and hnRNP-H, and leads to alterations in the splicing of secondary genes in muscle (24, 32, 33). DM2 is caused by a CCUG expansion in the first intron of zing finger protein 9 (*ZNF9*) pre-mRNA and is also associated with similar alterations in splicing (34). Of note, splicing of the cardiac troponin T is altered leading to cardiac defects; the skeletal muscle-specific ClC-1 channel is altered causing muscle hyper-excitability, and the insulin receptor gene is altered to favor skipping of exon 11 (from 70% exon11+ to 20%) (24, 35, 36). The authors suggest that this latter alteration might explain the insulin-resistant phenotype in DM1, as it is not seen in other non-DM1 myopathies that do not exhibit insulin resistance.

We have previously defined intronic splicing enhancers and silencers in the intron 10 of human *INSR* pre-RNA and have shown that the CELF protein CUG-BP1 binds exonic and intronic silencer elements (37, 38). Here, we tested whether similar *cis*-elements might be present in the rat *INSR* gene and found that the homologous elements do not appear to regulate the rat gene. Subsequently, we identified an element in the downstream intron that is conserved across species and found that this element binds Mbnl1 to promote exon inclusion. Deletion of this element eliminates the stimulatory effect of Mbnl1 in HEK293 cells suggesting that this is the primary binding site of the Mbnl1 to regulate alternative splicing of the *INSR* gene. More interestingly, our results also suggest that the relative abundance of Mbnl1 and its antagonistic partner, CUG-BP1, might determine the expression of the splice variants of *INSR* isoform in a given cell or developmental stage.

EXPERIMENTAL PROCEDURES

Plasmid Constructs—The wild-type human *INSR* minigene (hIRB) has been described previously as minigene B (37). All other plasmids were constructed using standard techniques. The expression plasmid for Mbnl1, SRp20, was purchased from ATCC (Manassas, VA). The expression plasmid for CELF4 was a gift from Dr. Thomas Cooper (Baylor University, Houston, TX).

Cell Culture, Transfections, and RNA Extraction—Unless otherwise stated, all tissue culture media and supplements were purchased from Invitrogen. Human hepatoma liver cells (HepG2), rat hepatoma liver cells (Fao), and human embryonic kidney 293 (HEK293) cells were maintained routinely in minimum essential medium plus Earle's salts with 10% fetal bovine serum and gentamycin sulfate antibiotic at 37 °C under 10% CO_2. The day before transfection, cells were plated at a density of ~1 × 10^6 cells/well in 6-well dishes. Medium was changed

every 2 days. Transient transfections of cells with plasmid DNA were performed with TransFast reagent (Promega, Madison, WI) according to the manufacturer's protocol. For cotransfection experiments, cells were transfected with 500 ng of minigene plasmid DNA and 1 μg of an expression vector for splicing factors of interest. In a given experiment, the total amount of DNA was maintained constant by adding control vector. Cells were harvested 48 h after transfection, and total cellular RNA was prepared using RNAzol B (Tel-Test Inc., Friendswood, TX) following the manufacturer's directions and precipitated twice.

Reverse Transcription and Amplification of cDNA—To generate cDNA, total RNA (1.0 μg) was reverse-transcribed using MultiScribe Reverse Transcriptase (Applied Biosystem) and random primers. PCR amplification of IR splice products derived from the minigenes was performed as published previously (37) using minigene-specific primer sets. Spliced products from endogenous IR transcripts were detected by primers located outside the minigene construct. Spliced products were visualized on 12% polyacrylamide gels, stained with EtBr, and quantified using Kodak Electrophoresis Documentation and Analysis System 290. Results were confirmed by at least three independent experiments and expressed as percentage of IR-B.

Immobilization of RNA on Agarose Beads and RNA Binding Assays—Substrate RNAs for bead immobilization were chemically synthesized by Integrated DNA Technologies Inc. (Coralville, IA). RNA affinity chromatography was performed by modification of a published procedure (39). Briefly, 1000 pmol of RNA was oxidized with sodium *m*-periodate (Sigma) and covalently coupled to 400 μl of a 50% slurry of adipic acid dihydrazide-agarose beads (Sigma). The beads were washed three times with 2 M NaCl and then equilibrated with buffer D (20 mM HEPES-KOH, pH 7.6, 10% (v/v) glycerol, 150 mM KCl, 0.2 mM EDTA, 0.5 mM dithiothreitol). RNA-agarose bead slurry was incubated with 75 μl of HeLa nuclear extract under splicing conditions at 30 °C for 25 min in buffer D in a total volume of 600 μl. The beads were washed five times with buffer D. Bound proteins were then eluted by boiling in 60 μl of 2× SDS sample buffer. The affinity-selected proteins were electrophoresed on a 4–12% BisTris gel and analyzed by Western blotting.

Small Interfering RNA (siRNA) Transfectionss—Double-stranded, pre-annealed siRNA oligonucleotides against Mbnl1 and scrambled siRNA were purchased from Santa Cruz Biotechnology (Santa Cruz, CA). Transfections with si-Mbnl1 were performed in HepG2 using the TransFast reagent (Promega). The final siRNA concentration for transfection was 100 nM. Forty eight hours after transfections, cells were harvested and assayed for mRNA. To check protein expression, cells were harvested 72 h after transfection.

Whole Cell Lysate Preparation and Western Blot Analysis—Whole cell extracts were prepared by harvesting the HepG2, Fao, and HEK293 cells. Lysates were prepared by sonication in harvesting buffer (10 mM Tris, 1% SDS). Total proteins were quantified with DC protein assay kit (Bio-Rad) using bovine serum albumin as standard. Equal amounts of protein were resolved in 4–12% BisTris gels and transferred to polyvinyl difluoride membrane (Millipore, Bedford, MA). The mem-

branes were blocked with 3% nonfat dried milk in TBS-T (20 mM Tris, 150 mM NaCl, 0.1% Tween 20) and then exposed to the appropriate concentrations of primary antibodies overnight at 4 °C. The following primary antibodies were used: mouse monoclonal anti-Mbnl1 (1:3000; Sigma), mouse monoclonal CUG-BP1 (1:3000; Santa Cruz Biotechnology), and mouse monoclonal anti-β-tubulin (1:10,000; Santa Cruz Biotechnology). After washing with TBS-T, the membranes were incubated for 1 h with horseradish peroxidase-conjugated goat anti-mouse immunoglobulin G, and the proteins were detected by ECL plus Western blotting detection reagents (GE Healthcare). Results were confirmed by at least three independent experiments.

RNP Immunoprecipitation and RT-PCR—RNPs containing Mbnl1 were immunoprecipitated using the protocol described previously (40, 41) with required modifications. Briefly, HeLa cells were washed with cold phosphate-buffered saline and harvested from tissue culture plates with a rubber scraper after treatment with lysis buffer (100 mM KCl, 5 mM MgCl$_2$, 10 mM HEPES, pH 7.6, and 0.5% Nonidet P-40 with 1 mM dithiothreitol, 100 units/ml RNasin (Promega), and EDTA-free complete protease inhibitor mixture (Roche Applied Science)). The lysate was stored immediately at −80 °C to complete lysis process as well as preventing adventitious binding. At the time of use, the RNP lysate was thawed and clarified by centrifugation at 16,000 × g for 10 min at 4 °C. The lysate was diluted to 1 μg/μl protein with phosphate-buffered saline (no Ca^{2+} and no Mg^{2+}), and then mouse monoclonal anti-Mbnl1 antibody (3A4, Santa Cruz Biotechnology) or mouse IgG was added to 200 μl of the cell lysate. The reaction mixture was rotated at 4 °C overnight, and 30 μl of protein G-agarose beads (Upstate Chemicon, Temecula, CA) was then added and rotated for 2 h at 4 °C. The beads were washed five times with NT2 buffer (50 mM Tris-HCl, pH 7.4, 150 mM NaCl, 0.05% Nonidet P-40, 1 mM MgCl$_2$), and the immunoprecipitated proteins were eluted using 2× SDS sample buffer. Aliquots of the precipitated proteins were separated by SDS-PAGE and immunoblotted with anti-Mbnl1 antibodies to confirm the specificity of the immunoprecipitation.

Immunoprecipitated RNAs were recovered by proteinase K digestion (2 μg/μl, 37 °C, 30 min) of the precipitated proteins and subsequent RNAzol B extraction. RNA was treated with RQ1 DNase (Promega) to remove DNA. RNA was then reverse-transcribed using MultiScribe reverse transcriptase (Applied Biosystem) and random primers. The resulting cDNA was analyzed by PCR for *INSR* or *GAPDH*. PCR for *INSR* was carried out using primers flanking the Mbnl-binding sites in the intron 11 enhancer element (marked with *red arrows* in supplemental Fig. S4). Glyceraldehyde-3-phosphate dehydrogenase primers are sense 5′-GAAGGTGAAGGTCGGA-GTC-3′ and antisense 5′-GAAGATGGTGATGGGA-TTTC-3′.

Statistical Analysis—Statistics were analyzed by one-way ANOVA with Tukey post-tests for multiple comparisons or by two-tailed Student's t test for pairwise comparisons using Prizm 4 (GraphPad Software, La Jolla, CA).

RESULTS

Intronic Enhancer and Silencer in Intron 10 of Human Gene Are Not Present in the Rat Gene—We previously defined splicing silencer and enhancer sequences in intron 10 in the human *INSR* gene (37). The rat gene shows the same overall tissue-specific differences in exon 11 incorporation as the human gene (19 –21, 42, 43). Although exon sequences are generally conserved between species, intron sequences are not. Comparison of the GA-rich enhancer sequences in intron 10 of the human gene with the corresponding region from the rat, mouse, dog, and horse genes revealed weak overall conservation outside of a number of GGG motifs (supplemental Fig. S1). At the 3′ end of the intron, the polypyrimidine tract and branch point sequence are highly conserved, as is the intronic silencer element that binds CUG-BP1 (supplemental Fig. S2). Therefore, we investigated whether the homologous regions in the rat *Insr* gene are functionally equivalent to the human sequences. Initially, we undertook a comparison of the regulation of the rat and human insulin receptor genes utilizing a chimeric minigene approach. We generated chimeric minigenes containing homologous regions from the rat gene in place of the previously identified human splicing elements, and we determined the effect on splicing following transfection into HepG2 cells (Fig. 1). Replacement of the human GA-rich enhancer sequence with the rat sequence was able to partially restore splicing on a deleted human intron (Fig. 1, compare *hIRΔ2K* with *hΔ1.9r220*) although not to the level of the human sequence (Fig. 1, compare *hΔ1.9r220* with *hIRΔ1.9K*), but the rat sequence did not work on the full-length intron (Fig. 1, compare *hIRΔ103* with *hΔ103r220*). At the 3′ end of the intron, 53 nucleotides of the rat 3′ splice site were able to substitute for the human 3′ splice site (Fig. 1, compare *hIRΔ67* with *hΔ119r53*). Interestingly when substituted into the full intron, the rat 3′ splice site promoted higher exon inclusion than the human sequence (Fig. 1, compare *hIRr53* with *hIRB*). We have published previously that the human sequence is predicted to form a stable stem-loop structure with exon 11 (38). The rat and human sequences have eight nucleotide differences that would disrupt the stem region, so it is unlikely that the rat 3′ splice site would form a stable secondary structure. We have shown previously that mutation of four nucleotides in this stem region renders exon 11 constitutive in the human minigene (38), which is consistent with the increased exon inclusion in hIRr53. Deletion of the human intronic silencer, including the CUG-BP1-binding site, in the presence of the rat 3′ splice site did not further increase exon inclusion (Fig. 1, compare *hΔ119r53* with *hIRr53*) as the exon is already efficiently included. Similarly, inclusion of the homologous rat silencer did not decrease exon inclusion (Fig. 1, compare *hΔ119r53* with *hΔ119r162*). Increasing the length of the substituted rat sequence caused a decrease in exon incorporation (compare *hΔ119r53* with *hΔ119r470*), but this could be a spacing effect due to the extra 400 nucleotides. Thus, we conclude that only the rat 3′ splice site can fully substitute for the human sequence.

To test the function of the rat elements in the context of the rat *Insr* gene, we created a rat minigene that had a similar structure to the human minigene, containing exons 10 –12, the com-
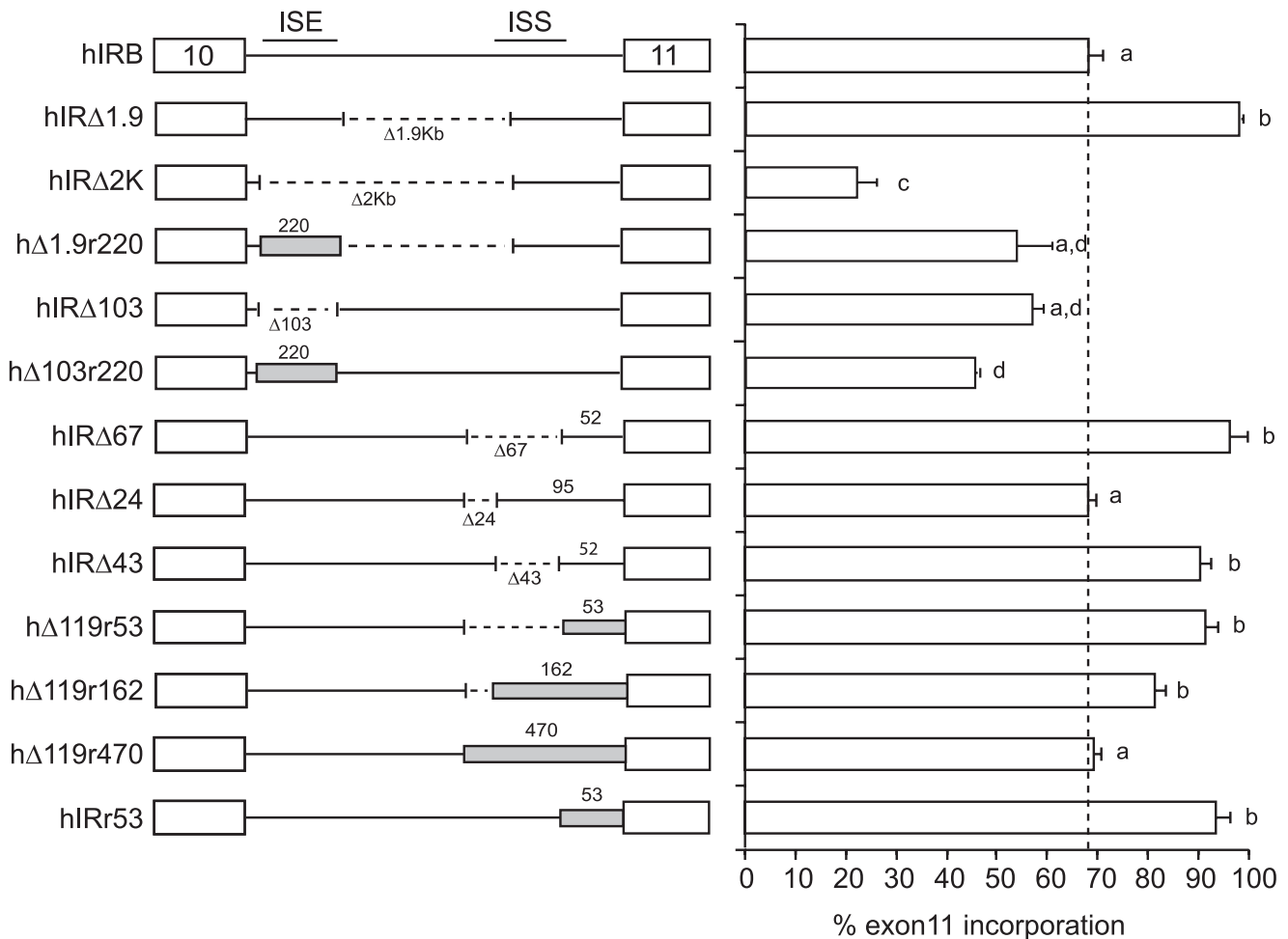
FIGURE 1. **Homologous rat sequences can partially substitute for the intronic enhancer but not the silencer in intron 10 of human gene.** Schematic diagram of human IR minigene chimeras with rat sequence substitutions is shown on *left*. *White boxes* represent human exons 10 and 11 separated by intron 10. *Dotted lines* indicate deletions in the intervening intron. *Gray boxes* indicate the homologous sequence from the rat *Insr* gene. *Numbers below* the introns indicate sizes of deletions. *Numbers above* the intron and *gray boxes* indicate length of human or rat sequence. The positions of the human intronic splicing enhancer (*ISE*) or silencer (*ISS*) are indicated in hIRB. These minigenes were transfected into HepG2 cells. Total RNA was isolated 48 h post-transfection and was subjected to RT-PCR analysis using primers specific to the transfected IR minigene mRNA. The mean ± S.E. for percent exon 11 inclusion is shown as a *bar graph* on the *right*. Results are derived from at least three independent experiments. Statistical significance was analyzed by ANOVA. *Bars* with the *same letter* are not significantly different ($p < 0.05$).

plete intron 10, and a deleted intron 11. The putative enhancer and silencer elements were deleted from the rat minigene. The minigenes were tested by transfection into the human HepG2 hepatoma cells as before for the human minigenes and also into the rat Fao hepatoma cells to provide a homologous system. Deletion of GA-rich region from the rat gene had no effect in either HepG2 or Fao cells (Fig. 2, *rIRΔ220*). Similarly, deletion of the 3′ silencer did not alter exon inclusion (Fig. 2, *rIRΔ310, Δ618*, or *Δ727*). A similar series of deletions was made in a minigene containing 1 and 1.9 kb at the 5′ and 3′ ends of the downstream intron (rIRP), respectively. Inclusion of the extra intronic sequence decreased exon 11 inclusion in both HepG2 and Fao cells (Fig. 2, compare *rIR* with *rIRP*), but the internal deletions had no further effect. Thus, the rat sequences do not appear to have the same enhancer and silencer functions as in the human *INSR* gene.

Comparison of the Rat and Human Insulin Receptor Genes Identifies a Downstream Intronic Splicing Enhancer—Based on proximity arguments, increasing the spacing of the distal splice site should increase exon inclusion, but increasing the

length of intron 11 decreased exon inclusion in both HepG2 cells and Fao cells (Fig. 2). Consequently, we investigated whether the downstream intron of the rat *Insr* gene might contain splicing regulatory elements. Minigenes were created that contained portions of the downstream intron from the rat gene and were tested in both human HepG2 and rat Fao hepatoma cells (Fig. 3). Deletion of 2.7 kb of intron 11 increased exon incorporation as seen before (Fig. 3*A*, compare *rIRP* with *rIR*) suggesting a potential silencer element. Adding back 1.9 kb of the 3′ end of the intron strongly repressed exon 11 inclusion in both HepG2 and Fao cells (Fig. 3*A*, compare *rIR1.9K* with *rIR*). This suggests that the 3′ end contains an element that promotes distal splice site use. An additional 190 nt at the 5′ end of the intron in this minigene caused a dramatic increase in exon 11 inclusion in Fao cells only (Fig. 3*A*, compare *rIR1.9K* with *rIR290/1.9K*) suggesting a possible Fao-specific splicing enhancer within this 190-nt region. In contrast, adding back 1 kb at the 5′ end of the deleted intron increased exon inclusion (Fig. 3*A*, compare *rIR* with *rIR1K* and *rIR1K/250*), although the effect was
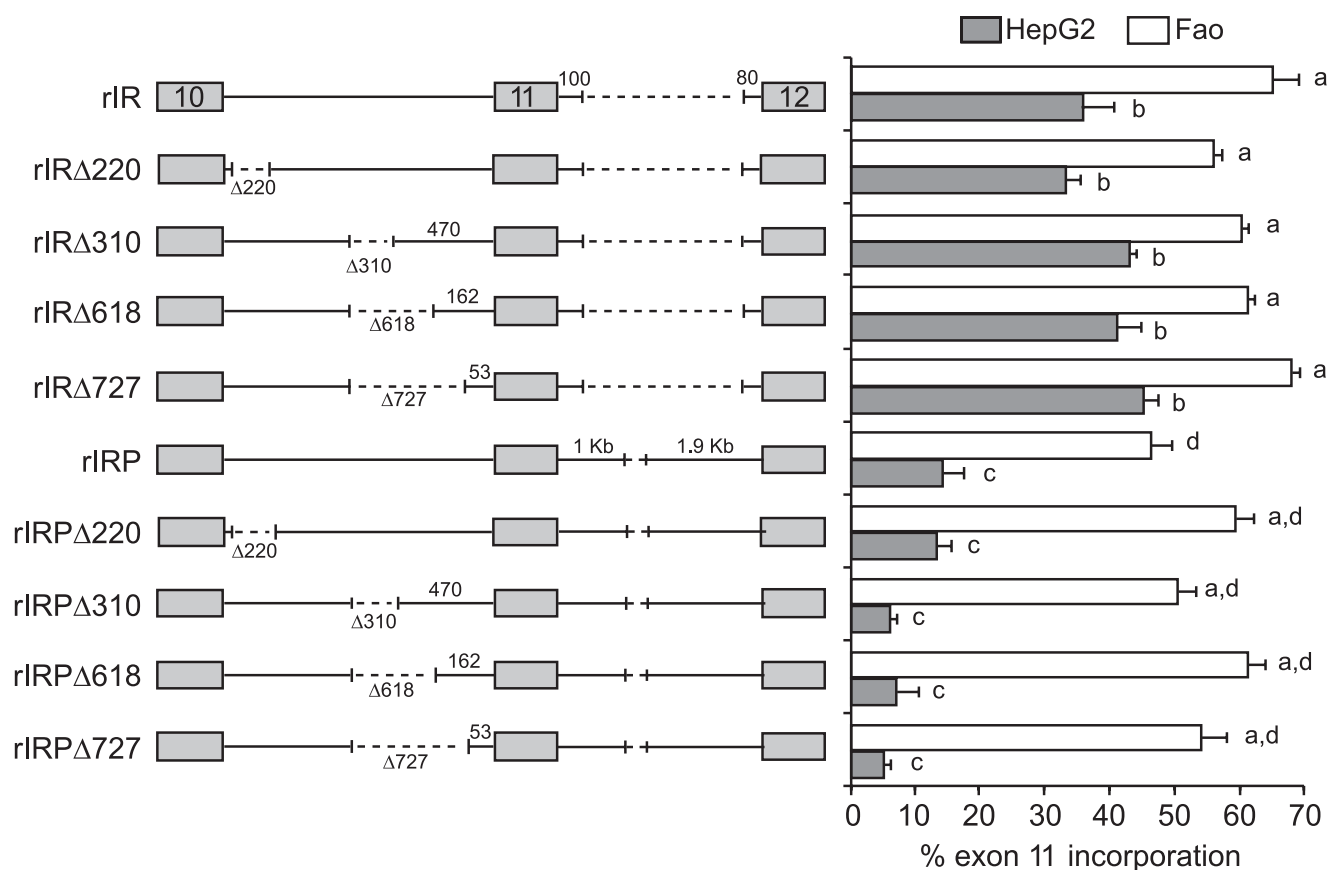
FIGURE 2. **Rat sequences do not appear to have enhancer and silencer functions in the rat *Insr* gene.** Schematic diagram of rat IR minigenes is shown on *left*. *Gray boxes* denote exons 10–12, and *intervening lines* indicate the introns in-between. *Dotted lines* indicate deletions. *Numbers below* the introns indicate sizes of deletions. *Numbers above* the lines indicate length of rat intron sequence. These minigenes were transfected into HepG2 and Fao cells, and IR minigene splicing was assessed as before. The mean ± S.E. for percent exon 11 inclusion in HepG2 (*gray bar*) and Fao cells (*white bar*) is shown as a *bar graph* on the *right*. Results are derived from at least three independent experiments and are given as mean ± S.E. Statistical significance was analyzed by ANOVA for each cell line independently. *Bars* with the *same letter* are not significantly different ($p < 0.05$).

much less dramatic than in the presence of the element in the 3′ end of the intron (Fig. 3*A*, compare *rIR1.9K* with *rIR290/1.9K*).

The rat intron 11 deletion mutants suggested the presence of a splicing enhancer within a 190-nt region at the 5′ end of the intron. A comparison of the sequences of exons 11 and 12 of human, rhesus monkey, dog, horse, mouse, and chicken *INSR* genes showed that the exons are highly conserved but the introns are not (supplemental Fig. S3). Intriguingly, intron 11 immediately downstream of exon 11 has an ~200-nt region of cross-species homology. The exception is the chicken *INSR* gene, which does not encode an exon 11. An 800-nt region covering exon 11 and the ends of the adjacent introns is shown in the Vista alignment plot (Fig. 3*B*). The 190-nucleotide intronic fragment with enhancer activity described above is contained in the region with homology to the human intron (supplemental Fig. S3).

The human minigene, hIRB, contains 184 nucleotides of the 5′ end of intron 11, which contains part of the homology region, so we created a rat minigene containing the rat 190-nucleotide equivalent in the deleted intron (rIR). This insertion increased exon incorporation in Fao cells but not HepG2 cells (Fig. 4*A*, compare *rIR5′190* with *rIR*). Insertion of a similarly sized fragment from the 3′ end (rIR3′170) did not increase exon inclusion in either cell. We then inserted the entire 169-nt region of

homology from the rat *Insr* gene in the correct or reversed orientation in the rat minigene. Addition of one or two copies of the conserved element increased exon incorporation in HepG2 and Fao cells (Fig. 4*A*, compare *rIR* with *rIR+enh* and *rIR+2enh*). Interestingly, this element functioned as an enhancer in both HepG2 and Fao cells. Addition of the enhancer element in reverse orientation (rIR+enhrev) does not have any stimulatory effect. As a control, we incorporated a similar length of sequence from the 3′ end of intron 11 in forward (rIR+3′end) or reverse (rIR+3′endrev) orientation. Both of these constructs have no stimulatory effect. Similar human minigenes were constructed. The 5′ end of intron 11 was deleted to remove the entire region of homology resulting in decreased exon 11 inclusion (Fig. 4*B*, compare *hIRΔ164* with *hIRB*). The entire 175-nt region of homology was added back resulting in increased exon inclusion in both Fao and HepG2 cells (Fig. 4*B*, compare *hIR+enh* with *hIRΔ164*). Addition of an equivalent region from the 3′ end of the intron to the partial enhancer in hIRB had no effect. These findings demonstrate that the species-conserved region indeed functions as a splicing enhancer in both genes.

Downstream Intronic Splicing Enhancer Binds Mbnl1 in Vitro and in Vivo—Sequence analysis of the conserved sequence for potential splicing factor recognition sites indicated multiple sites for Mbnl1 (supplemental Fig. S4). Mbnl1
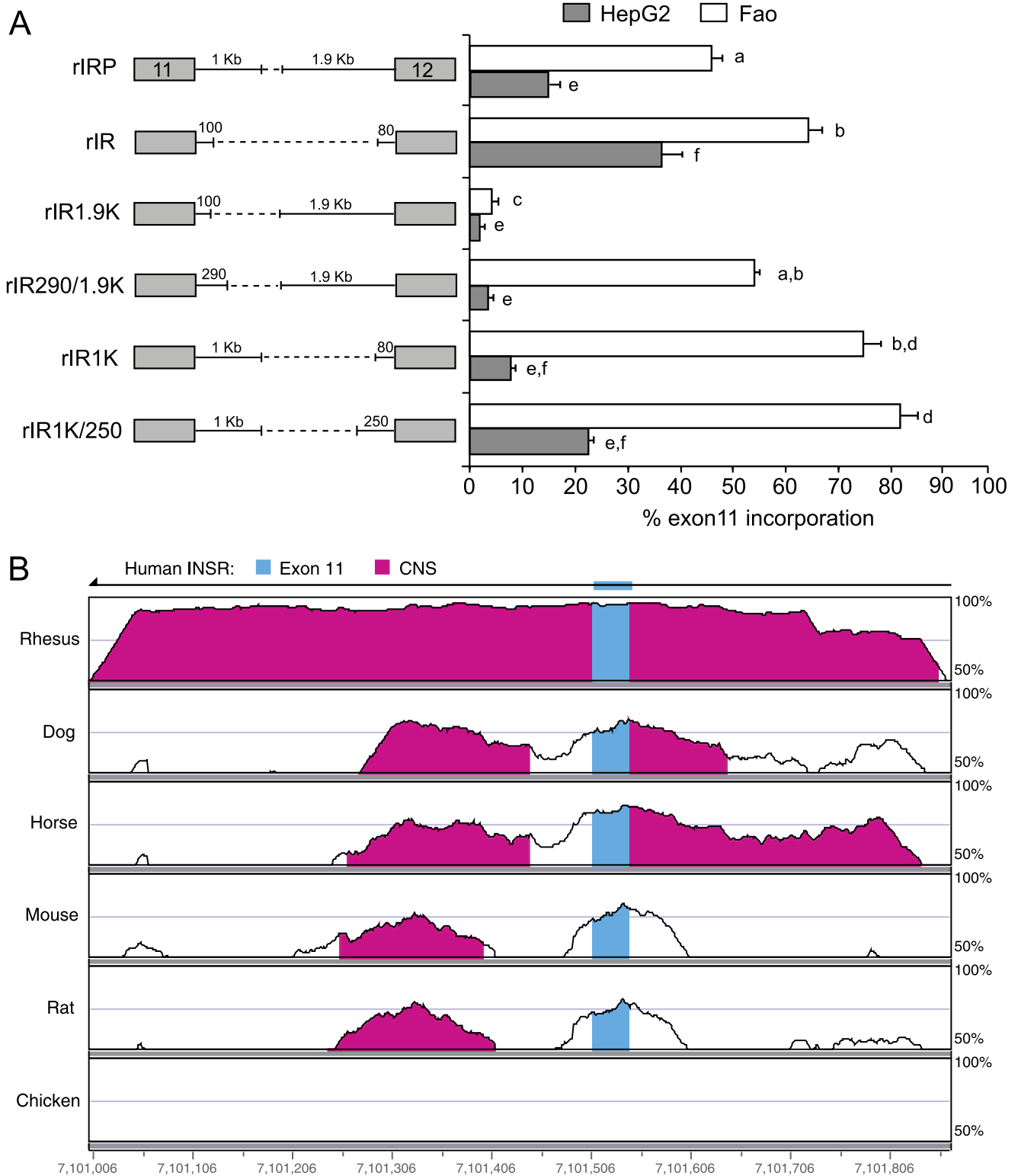
FIGURE 3. **Comparison of the rat and human *INSR* genes identifies a conserved downstream splicing element.** *A,* schematic of rat IR minigene deletion mutants transfected into HepG2 and Fao cells. *Numbers above* the lines indicate length of rat intron sequence. Percent of exon 11 inclusion in HepG2 (*gray bar*) and Fao cells (*white bar*) is shown in the *bar graph* on the *right*. Results are derived from three independent experiments and are given as mean ± S.E. Statistical significance was analyzed by ANOVA for each cell line independently. *Bars* with the *same letter* are not significantly different ($p < 0.05$). *B,* vista alignment plot of human, rhesus monkey, dog, horse, mouse, rat, and chicken genomic sequences covering 800 nucleotides, including exon 11 and the ends of introns 10 and 11. Exonic structure of the human *INSR* gene is shown at the *top*. The gene reads from *right to left* as indicated by the *arrow* at the top, so intron 11 is to the *left* of exon 11. *Blue areas* indicate exon 11, and *magenta areas* indicate conserved nucleotide sequence (*CNS*) between the seven genomes. Conservation in these regions exceeds 50%. The chicken *INSR* gene does not contain an exon 11 and only encodes a single insulin receptor.
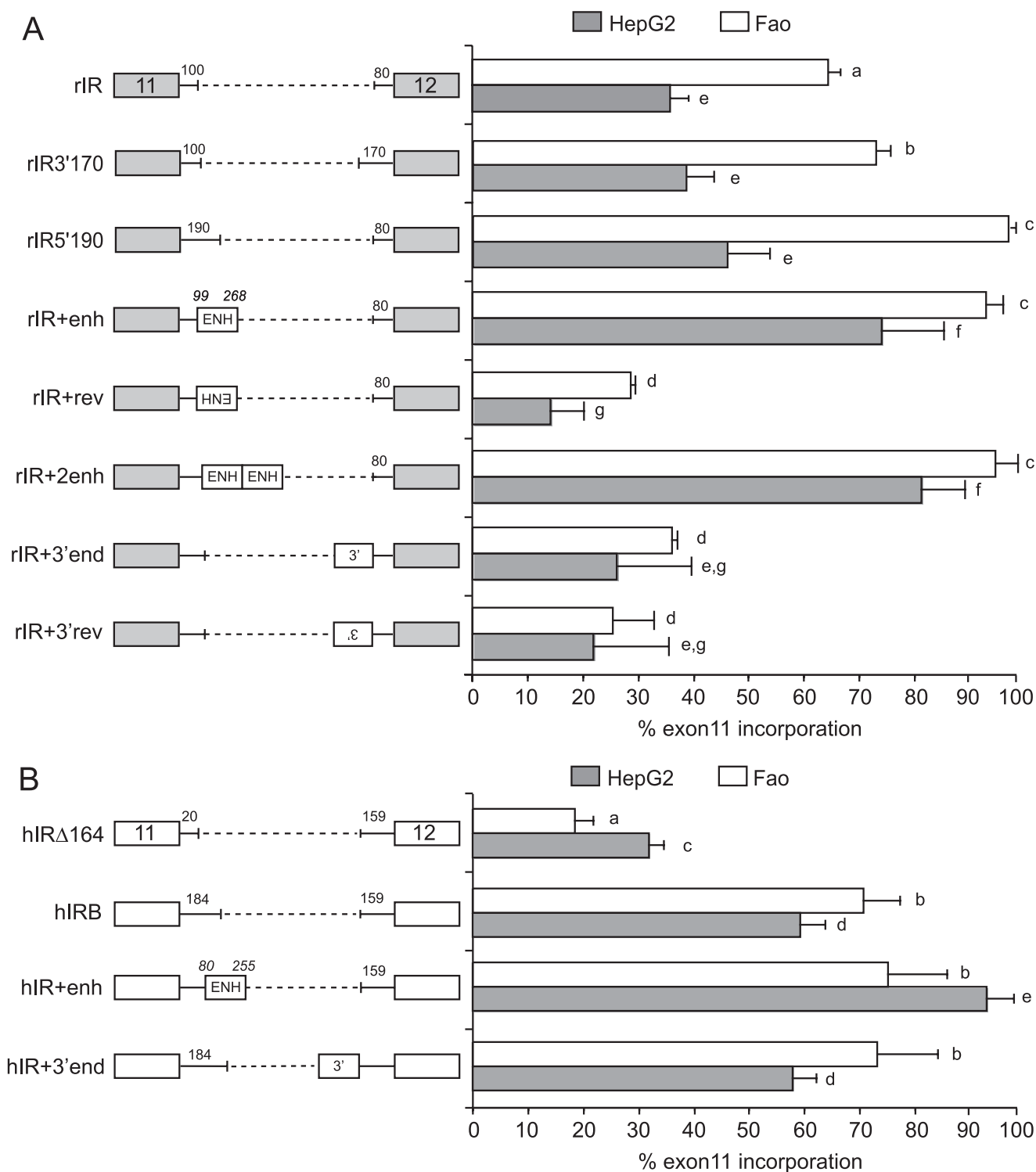
FIGURE 4. **Conserved intronic sequence is a splicing enhancer.** *A,* schematic diagram of rat IR minigenes is shown on the *left. B,* schematic diagram of human IR minigenes is shown on the *left.* For both panels, *gray boxes* denote rat exons 11 and 12, and *white boxes* denote human exons 11 and 12, and *intervening lines* indicate the introns in-between. *Dotted lines* indicate deletions. *Numbers above* the lines indicate length of rat intron sequence. Conserved enhancer region is indicated by *boxes* marked *ENH. Italicized numbers* indicate start and end of conserved region relative to the start of the intron in either the rat or human gene. Human HepG2 or rat Fao hepatoma cells were transiently transfected with these minigenes, and splicing was assessed as before. Percent of exon 11 inclusion in HepG2 (*gray bar*) and Fao cells (*white bar*) is shown as a *bar graph* on the *right.* Results are derived from at least three independent experiments and are given as mean ± S.E. Statistical significance was analyzed by ANOVA for each cell line independently. *Bars* with the *same letter* are not significantly different ($p < 0.05$).

can recognize pathogenic CUG expansions, but its normal targets are less well defined. Three groups have shown that Mbnl1 recognizes YGCU(U/G)Y motifs in the *TNNT2, TNNT3,* and

SERCA1 genes (44–47). A recent study also demonstrated that Mbnl1 binds YGCY motifs to regulate alternative splicing (48). Mbnl1 also binds to this motif when present in a stem-loop
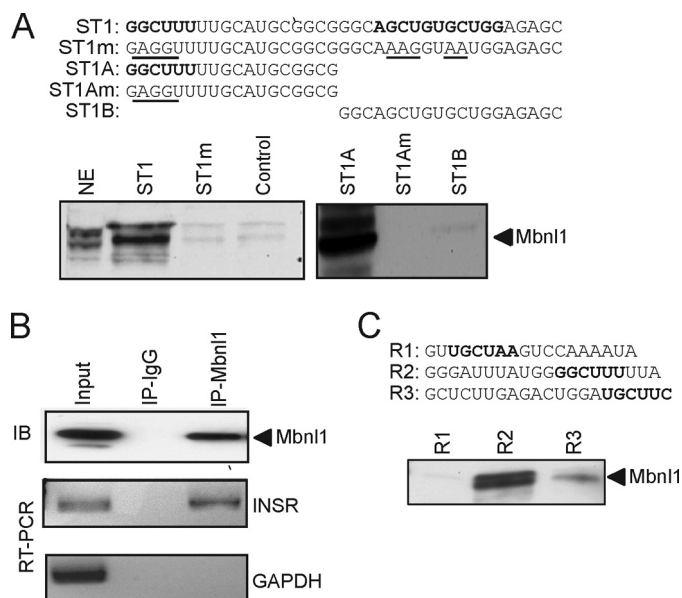
FIGURE 5. Mbnl1 binds to the insulin receptor RNA both *in vitro* and *in vivo*. *A,* sequences of the RNA oligonucleotides, derived from human intron 11, used for RNA affinity purification. Putative Mbnl1-binding sites are marked in boldface, and mutations are *underlined*. RNA oligonucleotides were covalently linked to adipic acid dihydrazide-agarose beads. HeLa nuclear extracts were incubated with the beads and washed extensively, and then associated proteins were eluted with SDS-PAGE sample buffer. Bound proteins were separated on 4–12% BisTris gels and immunoblotted with anti-Mbnl1. *NE* indicates input HeLa nuclear extract (1/25th of input). Representative blots are shown. Experiment was repeated five times with similar results. *B,* intracellular association between Mbnl1 and the endogenous *INSR* transcript was analyzed by ribonucleoprotein immunoprecipitation. Endogenous Mbnl1 was immunoprecipitated (*IP*). Immunoblot (*IB*) shows that Mbnl1 protein is immunoprecipitated by anti-Mbnl1 antibody but not by mouse IgG (*upper panel*). RT-PCR assay shows that IR mRNA is coimmunoprecipitated by anti-Mbnl1 antibodies but not by IgG (*middle panel*). RT-PCR assay for control glyceraldehyde-3-phosphate dehydrogenase (*GAPDH*) mRNA (*lower panel*) is shown. *C,* sequences of the RNA oligonucleotides derived from rat intron 11 used for RNA affinity purification. Putative Mbnl1-binding sites are marked *boldface*. Representative Western blot for Mbnl1 is shown.

structure (44, 47). Potential Mbnl1-binding sites, both YGCY (highlighted in *blue* in supplemental Fig. S4) and YGCU(U/G)Y (highlighted in *green* in supplemental Fig. S4), are clustered within the region of homology in intron 11.

We analyzed Mbnl1 protein binding to the conserved element in human intron 11 by RNA affinity purification. For this, we synthesized a 37-nucleotide RNA (ST1) that contains three potential Mbnl1-binding sites as follows: GGCUUU, AGCUGU, and UGCUGG. We also synthesized a mutant RNA substituting each conserved GCU in the binding site (ST1m). As a negative control, we used random RNA oligonucleotides of similar length. These RNA oligonucleotides were coupled to adipic acid dihydrazide-agarose beads and used to affinity-purify splicing factors from HeLa cell nuclear extracts. Nuclear proteins bound to the RNA templates were analyzed by SDS-PAGE and immunoblotting with Mbnl1-specific monoclonal antibody. The 42-kDa Mbnl1 protein binds strongly to the wild-type RNA (Fig. 5*A*), but binding was not found on the mutant RNA or on the negative control (Fig. 5*A*). To further localize the Mbnl1-binding site, we performed the RNA affinity purification assay again using RNA templates containing each half of ST1 (ST1A and ST1B). Interestingly, Mbnl1 appears to bind to

the 5′-half ST1A (Fig. 5*A*) but not the 3′-half ST1B. Mutation in the GCU in the putative binding site in ST1A eliminates Mbnl1 binding (Fig. 5*A*, *ST1Am*). Recombinant full-length Mbnl1(1–382) can be expressed as a His-tagged protein in *Escherichia coli* and retains RNA binding (47). Therefore, we expressed recombinant Mbnl1 as a His-tagged protein and found that it also binds directly to the ST1 RNA template using our *in vitro* RNA affinity assay (data not shown).

The *in vitro* binding prompted us to determine whether Mbnl1 binds the endogenous *INSR* transcript RNA. We performed ribonucleoprotein immunoprecipitation analysis to pull down intracellular RNA-protein complexes. We utilized the HeLa cell line as it expresses endogenous Mbnl1, and the HeLa nuclear extract was used for *in vitro* binding assay. Mbnl1 immunoprecipitates were immunoblotted using an anti-Mbnl1 antibody. The Mbnl1 protein was precipitated with the Mbnl1 antibody but not in control mouse IgG immunoprecipitations (Fig. 5*B*). The immunoprecipitated samples were analyzed for specific RNA content by RT-PCR analysis. *INSR* intron 11 RNA was detected only in the Mbnl1 immunoprecipitate (Fig. 5*B*). Importantly, this association is specific because control glyceraldehyde-3-phosphate dehydrogenase RNA was not precipitated under the same conditions (Fig. 5*B*, *lower panel, lane 3*).

To test Mbnl1 binding to the homologous rat intron sequence, we synthesized three RNA oligonucleotides, R1, R2, and R3, containing YGCY motifs and used them for RNA affinity purification assay as for human RNA templates. We found that Mbnl1 binds strongly to the R2 sequence, which contains the identical GGCUUU motif found to bind Mbnl1 in the human ST1A sequence. Weaker binding was also seen in the R3 sequence, but Mbnl1 does not bind to the R1 sequence. This confirmed that Mbnl1 binds both the human and rat sequence and further suggested that the GGCUUU motif might be the major Mbnl1-binding site.

Mbnl and CELF Proteins Regulate the Inclusion of IR Exon 11— The Mbnl family of proteins has been shown to promote exon 11 incorporation in normal myoblasts, HEK293 and HeLa cells (45, 49). To examine whether Mbnl family members also regulate IR exon 11 splicing in rat and human hepatoma cells, minigene reporter constructs were transfected into HepG2, HEK293, and Fao cells with different protein expression vectors (Fig. 6*A*). We used the hIRB minigene to study the Mbnl1 effect in HepG2 and HEK293 cells as addition of full enhancer (hIR+enh) renders the exon constitutive, which would preclude observing any Mbnl1 effects. The hIRB minigene shows 65 and 28% exon 11 incorporation in HepG2 and HEK293 cells, respectively (Fig. 6*A*). Overexpression of Mbnl1 or -3, but not Mbnl2 or CELF4, increased exon 11 incorporation significantly in HepG2 cells (Fig. 6*A*). The findings were similar in HEK293 cells. The rat minigenes were transfected into the Fao cells. rIRP shows 35% exon 11 inclusion in Fao cells (Fig. 6*A*). Overexpression of Mbnl1–3, or CELF4 led to a significant increase in exon 11 inclusion (Fig. 6*A*). There were noticeable differences between the human and rat systems. In Fao cells, the Mbnl proteins did not increase exon 11 incorporation as dramatically as in HEK293 cells. Furthermore, overexpression of CELF4
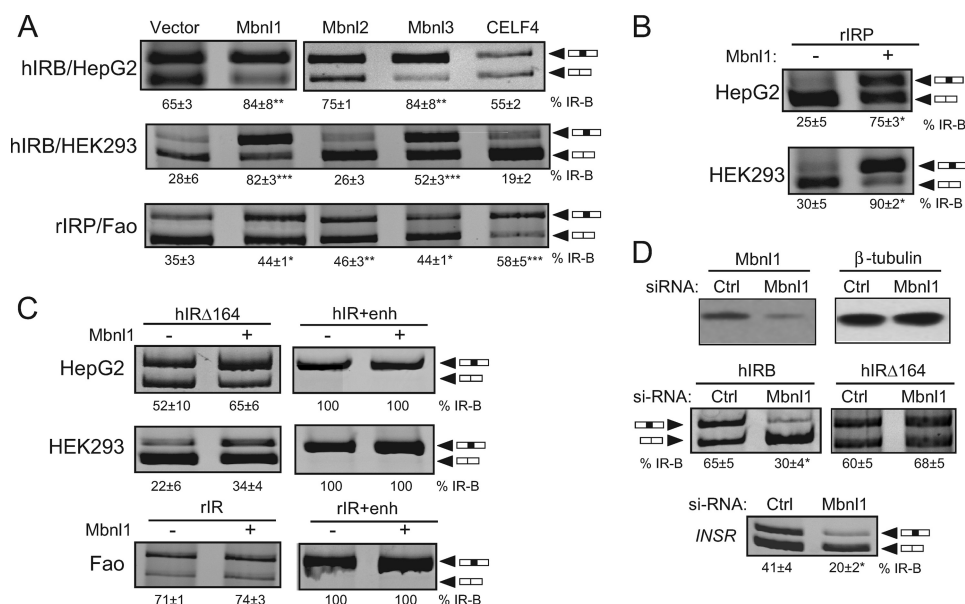
FIGURE 6. **Mbnl1 increases exon 11 incorporation through the downstream intronic enhancer element.** *A,* regulation of IR minigene splicing by Mbnl and CELF4. hIRB minigene was transfected into human HepG2 and HEK293 cells. The rat rIRP minigene was transfected into rat Fao hepatoma cells. Minigenes were cotransfected with the indicated expression vectors for Mbnl1, Mbnl2, Mbnl3, CELF4, or control pCMV vector. Spliced products were analyzed by RT-PCR as before. A representative gel is shown. The percentage of exon 11 inclusion (% IR-B ± S.D., $n = 3$) is shown *below* the gel. Statistical analysis was performed by ANOVA. *Asterisks* indicate statistical significance (*, $p < 0.05$; **, $p < 0.01$; ***, $p < 0.001$ *versus* vector) from three to four independent experiments. *B,* regulation of rat rIRP splicing regulation in human cell lines by Mbnl1. Rat rIRP minigene was cotransfected into HepG2 and HEK293 cells with or without the Mbnl1 expression vector. A representative gel is shown. The percentage of exon 11 inclusion (% IR-B ± S.D., $n = 4$) is shown *below* the gel. Statistical analysis was performed by *t* test in comparison with the empty pCMV vector. *Asterisks* indicate statistical significance (*, $p < 0.05$). *C,* regulation of human and rat IR minigenes with or without full enhancer element by Mbnl1. Minigenes were cotransfected with Mbnl1 in human and rat cell lines as before. Spliced products were analyzed by RT-PCR. A representative gel is shown. The percentage of exon 11 inclusion (% IR-B ± S.D., $n = 3$) is shown *below* the gel. Statistical analysis was performed by *t* test in comparison with the empty pCMV vector. *Asterisks* indicate statistical significance (*, $p < 0.05$). *D,* knockdown of Mbnl1. hIRB or hIRΔ164 minigenes were cotransfected with 100 nM siRNAs directed against Mbnl1 or scrambled control (*Ctrl*) siRNA in HepG2 cells. Mbnl1 protein content was measured by immunoblotting with anti-Mbnl1 monoclonal antibodies (*upper panels*). Blot was stripped and reprobed for β-tubulin protein expression as an internal control. Representative RT-PCR analysis of the exon 11 spliced products from minigene RNA (*middle panels*) or the endogenous *INSR* transcript (*bottom panel*) in Mbnl1 knockdown cells. The percentage of exon 11 inclusion (% IR-B ± S.D., $n = 3$) is shown. *Asterisks* indicate statistical significance (*, $p < 0.05$) *versus* scrambled siRNA control.

shown). As shown earlier, addition of the full enhancer element causes constitutive exon 11 inclusion so overexpression of Mbnl1 has no effect (Fig. 6*C*). We performed a similar analysis with the rat minigenes in Fao cells. Exon 11 inclusion for the rIR minigene that lacks the conserved element was completely unaffected by overexpression of Mbnl1. Insertion of the full enhancer in the deleted intron in rIR+enh again renders the exon constitutive and prevents any further Mbnl effect (Fig. 6*C*). Collectively, these results demonstrate that the deletion of the conserved enhancer element eliminates Mbnl1 responsiveness in both human and rat minigene constructs.

Knockdown of Endogenous Mbnl1 Decreases Inclusion of Exon 11 in HepG2 Cells—To confirm the role of endogenous Mbnl1 in alternative splicing of exon 11, we used RNA interference to knock down Mbnl1. For these experiments, we used the HepG2 cells as these cells express Mbnl1 and efficiently include exon 11. HepG2 cells were treated with Mbnl1 siRNA, and protein levels were quantified 72 h after transfection. Mbnl1 protein was reduced by 65% (Fig. 6*D, top panels*). To determine whether knockdown of Mbnl1 affects IR splicing, siRNA was cotransfected into HepG2 cells with the wild-type IR minigene (Fig. 6*D, middle panels*). Knockdown of Mbnl1 led to a 50% decrease in exon 11 incorporation in cells treated with siMbnl1 compared with the level in cells treated with control siRNA. In contrast, Mbnl1 knockdown had no effect on hIRΔ164 minigene splicing in HepG2 cells as this minigene lacks the enhancer-binding site for Mbnl1. The effect of the Mbnl1 knockdown was also observed on splicing of the endogenous *INSR* gene transcript. Treatment with si-Mbnl1 significantly decreased exon 11 incorporation from 41 to 20% (Fig. 6*D, bottom panel*).

Mbnl1 and SR Proteins Act Independently to Promote Exon 11 Inclusions—We have previously shown that SRp20 and SF2/ASF are required for exon inclusion in the *INSR* gene (38). To test whether the enhancing effect of Mbnl1 requires these SR proteins, we transfected cells with minigenes containing linker scanning mutations at the SRp20 or SF2/ASF sites (LS2 and LS5, respectively). Elimination of SR protein binding did not prevent the ability of Mbnl1 to increase exon inclusion (Fig. 7*A*). Conversely, we transfected SRp20 with the hIRΔ164 minigene lacking the Mbnl1-binding site. We observed that SRp20 significantly increases exon inclusion in the hIRΔ164 minigene,

increases exon incorporation in Fao cells but has the opposite effect in HepG2 and HEK293 cells, where it tended to decrease exon inclusion. This could reflect a difference in the rat and human minigenes or in the cell line used. Therefore, we transfected the rIRP minigene into both HepG2 and HEK293 cell lines. rIRP showed similar levels of exon 11 inclusion in the human HepG2 and HEK293 cells as in the rat Fao cells (Fig. 6*B*). Mbnl1 overexpression with the rat rIRP in HepG2 and HEK293 cells drastically increased exon 11 incorporation similar to the human minigene (Fig. 6*B*) suggesting that the differences are more related to cell type rather than minigene origin.

Mbnl Increases Exon 11 Incorporation through the Downstream Intronic Enhancer Element—To examine whether the observed Mbnl1 effect is due to binding to the conserved enhancer, we transfected hIR minigenes containing or lacking the enhancer into HepG2 and HEK293 cells with or without expression plasmids for Mbnl1. Deletion of the conserved enhancer in hIRΔ164 eliminated the ability of Mbnl1 to stimulate exon inclusion in both HepG2 and HEK293 cells (Fig. 6*C*). The hIRΔ164 minigene is also nonresponsive to overexpression of Mbnl2 and -3 in HepG2 and Mbnl3 in HEK293 (data not shown). As shown earlier, addition the wild-type IR minigene (Fig. 6*D, middle panels*). Knockdown
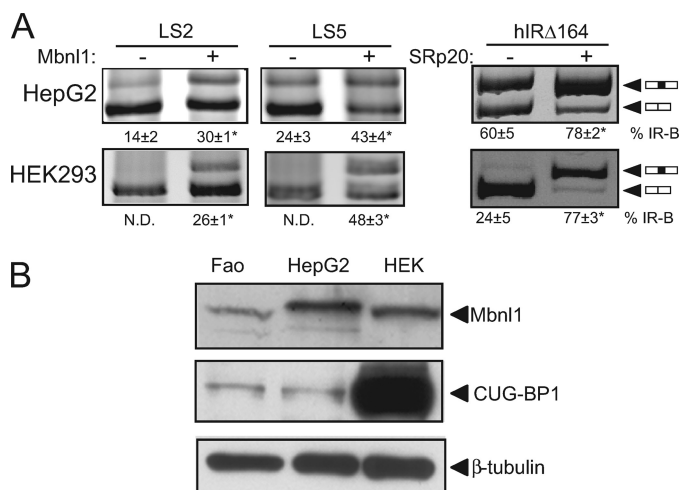
FIGURE 7. **Mbnl1 and SR proteins act independently to promote exon 11 inclusion.** *A,* linker scanning LS2 or LS5 mutant minigene constructs were cotransfected with the Mbnl1 protein expression vector into HepG2 (*upper panel*) and HEK293 (*lower panel*) cells. hIRΔ164 deletion mutant was cotransfected with the SRp20 protein expression vector. Spliced products were analyzed as before. The mean percentage exon 11 inclusion (% IR-B ± S.D., *n* = 3) is shown. *Asterisks* indicate statistical significance (*p* < 0.05) *versus* empty vector control. *N.D.,* not detectable. *B,* total cellular protein was extracted from Fao, HepG2, and HEK293 cells. Equal amounts of protein were loaded and immunoblotted for Mbnl1 and CUG-BP1. Blot was reprobed with β-tubulin as a loading control.

suggesting that Mbnl1 and the SR proteins have independent stimulatory effects to promoter exon inclusion. Furthermore, we were unable to document an interaction with SRp20 or SF2/ASF by coimmunoprecipitation or pulldown with recombinant Mbnl1, although we were able to confirm the known interaction of Mbnl1 and hnRNP-H (data not shown). This again suggested that the stimulatory effects of SR proteins and Mbnl proteins are independent and do not require direct protein-protein interactions.

Relative Abundance of Mbnl1 and CUG-BP1 Correlates with INSR Splicing Pattern—In human HepG2 and rat Fao hepatoma cells, exon 11 incorporation is significantly higher than human HEK293 embryonic kidney cells where exon 11 is predominantly skipped. The Mbnl and CUG-BP families have antagonistic effects on the alternative splicing of many genes. We have shown previously that CUG-BP1 represses exon 11 inclusion, and we show here that Mbnl1 promotes exon inclusion. Therefore, we measured Mbnl1 and CUG-BP1 protein levels in these cell lines. Although Mbnl1 is expressed at comparable levels in these cells, CUG-BP1 is expressed at a much higher level in HEK293 cells (Fig. 7*B*). Thus, relative abundance of these two splicing factors correlates with exon 11 skipping in the *INSR* gene.

DISCUSSION

Regulation of IR alternative splicing is critical to maintain the correct insulin receptor isoform ratio and hence correct insulin/insulin-like growth factor-II sensitivity. Here, we describe a novel intronic *cis*-element, which is located in the intron downstream of alternatively spliced exon 11. This element was identified by a combination of chimeric minigene and deletional analysis coupled with assessment of evolutionary sequence conservation. This intronic element is conserved across

human, horse, dog, mouse, and rat and acts as an enhancer in human and rat. Sequence analysis of this element identified multiple potential Mbnl1-binding sites, and we documented the ability of Mbnl1 to bind the enhancer *in vitro* and *in vivo*. We showed that Mbnl family members enhance exon 11 inclusion in hepatoma and HEK293 cells and that the intronic enhancer is required for Mbnl action. The results are somewhat different from published results in myoblasts (49). Overexpression of Mbnl1 or -2 in the muscle cells did not increase exon 11 inclusion, but knockdown of either Mbnl1 or -2 eliminated exon inclusion. It is possible that muscle cells express high levels of endogenous Mbnl proteins so overexpression does not lead to a further increase in exon inclusion.

A great deal of data has shown that *INSR* splicing is altered in myotonic dystrophy (49–51). The Mbnl proteins are functionally inactivated by binding to CUG and CCUG repeats resulting in increased expression of CUG-BP1 and hnRNP-H proteins (49). These changes culminate in reductions in exon 11 inclusion in the *INSR* gene. Interfering with the binding of Mbnl to the repeat expansions or overexpression of Mbnl reverses many splicing defects associated with myotonic dystrophy (52, 53). Most of these studies have been performed in muscle cells, as this is the site of *DMPK* and *ZNF9* gene expression, but Mbnl and CUG-BP1 proteins are expressed in many other tissues. Human Mbnl1 is more abundant in skeletal muscle and heart than brain, kidney, liver, and pancreas, but Mbnl2 shows similar expression in all tissues. Kalsotra *et al.* (7) have shown a postnatal switch in CUG-BP1 and Mbnl1 protein expression in the developing heart that underlies the embryonic/adult transition in splicing of many genes. This is consistent with the antagonistic effects of CELF and Mbnl family of proteins on *INSR* splicing. We have already identified two binding sites for CUG-BP1 in the *INSR* gene, one in exon 11 and the other upstream of the branchpoint sequence in intron 10 (38). Both sites appear to be required for the repression of exon 11 inclusion by CUG-BP1 as mutation of either element does not completely eliminate the inhibition. We proposed that CUG-BP1 represses exon inclusion by stabilizing RNA secondary structure and competing for SRp20 binding. In contrast, very little was known about the targets for Mbnl1 in the *INSR* gene despite good evidence for functional effects by Mbnl1 overexpression or knockdown. Mbnl1 is a zing finger protein containing four amino-terminal CCCH motifs ($CX_7CX_{4-6}CX_3H$) that recognize both single-stranded RNA and double-stranded RNA. Most of the known natural and pathogenic binding sites are found in regions of RNA secondary structure (47). Mbnl1 has a preference for the sequence YGCU(U/G)Y in the *TNNT3*, *TNNT3*, and *SERCA1b* genes (46). Multiple Mbnl1-binding sites lie downstream of exon 22 of the *SERCA1* gene, and Mbnl1 promotes exon 22 incorporation (46), so the location of the Mbnl1-binding sites downstream of the alternatively spliced IR exon 11 is consistent with the effect of Mbnl1 to increase exon 11 incorporation. Conversely, the Mbnl1-binding sites in the cTNT and *TNNT3* genes are upstream of the alternatively spliced exon (45, 47), and Mbnl1 suppresses exon incorporation in both cases. Goers *et al.* (48) also proposed a generalized model that Mbnl1-binding upstream of an exon is likely to cause silencing of the downstream splice site, whereas Mbnl1 binding downstream of an

exon is likely to enhance usage of the upstream splice site. A similar model has been proposed for the splicing factor NOVA1 (54).

How Mbnl1 regulates exon inclusion is still being explored. In cases where Mbnl1 promotes exon skipping, Mbnl1 has been shown to bind to 3′ splice sites and prevent recognition by U2AF65 (55). A genome-wide analysis of alternative splicing in multiple tissues has shown that Mbnl1 promotes exon inclusion, as it does for the *INSR* gene, by binding to downstream sites. Mbnl-binding motifs (UGCU) are found downstream of cassette exons that are up-regulated in skeletal muscle and heart, which is consistent with our finding for the *INSR*, but these same motifs are found upstream of cassette exons enriched in brain (56). Binding motifs for the CELF proteins are also found downstream of some cassette exons enriched in muscle but not heart. These studies all emphasize the importance of context for the functional effect of the Mbnl/CELF proteins. The presence of multiple binding sites in the *INSR* conserved enhancer element suggests that protein multimerization might be important for Mbnl1 activity. We identified strong Mbnl binding to a GGCUUU motif in both the human and the rat *INSR* genes, but many other potential binding sites are present. It is possible that these weaker sites are also occupied by Mbnl, as a result of protein multimerization in the context of the full enhancer. This would explain why the full enhancer is stronger than a partial enhancer that contains the GGCUUU motif. The notion of cooperative recognition of the enhancer is supported by the observation that knockdown of either Mbnl1 or Mbnl2 impairs exon inclusion in myoblasts (49). Finally, Mbnl proteins are not the only potential splicing factors recognizing the intronic enhancer as we have identified potential binding sites for Nova1 and Fox1/2 proteins. Further studies will be needed to determine the relative contributions of these factors.

REFERENCES

1. Wang, G. S., and Cooper, T. A. (2007) *Nat. Rev. Genet.* **8,** 749–761
2. López-Bigas, N., Audit, B., Ouzounis, C., Parra, G., and Guigó, R. (2005) *FEBS Lett.* **579,** 1900–1903
3. Krämer, A. (1996) *Annu. Rev. Biochem.* **65,** 367–409
4. Rio, D. C. (1992) *Curr. Opin. Cell Biol.* **4,** 444–452
5. Lopez, A. J. (1998) *Annu. Rev. Genet.* **32,** 279–305
6. Black, D. L. (2003) *Annu. Rev. Biochem.* **72,** 291–336
7. Kalsotra, A., Xiao, X., Ward, A. J., Castle, J. C., Johnson, J. M., Burge, C. B., and Cooper, T. A. (2008) *Proc. Natl. Acad. Sci. U.S.A.* **105,** 20333–20338
8. Gromak, N., Matlin, A. J., Cooper, T. A., and Smith, C. W. (2003) *RNA* **9,** 443–456
9. Izquierdo, J. M., Majós, N., Bonnal, S., Martínez, C., Castelo, R., Guigó, R., Bilbao, D., and Valcárcel, J. (2005) *Mol. Cell* **19,** 475–484
10. Martinez-Contreras, R., Cloutier, P., Shkreta, L., Fisette, J. F., Revil, T., and Chabot, B. (2007) *Adv. Exp. Med. Biol.* **623,** 123–147
11. Sanford, J. R., Ellis, J., and Cáceres, J. F. (2005) *Biochem. Soc. Trans.* **33,** 443–446
12. Ule, J., Jensen, K. B., Ruggiu, M., Mele, A., Ule, A., and Darnell, R. B. (2003) *Science* **302,** 1212–1215
13. Zhang, C., Zhang, Z., Castle, J., Sun, S., Johnson, J., Krainer, A. R., and Zhang, M. Q. (2008) *Genes Dev.* **22,** 2550–2563
14. Buratti, E., Baralle, M., and Baralle, F. E. (2006) *Nucleic Acids Res.* **34,** 3494–3510
15. Hiller, M., Zhang, Z., Backofen, R., and Stamm, S. (2007) *PLoS Genet.* **3,** e204
16. Graveley, B. R. (2005) *Cell* **123,** 65–73
17. Hernández-Sánchez, C., Mansilla, A., de Pablo, F., and Zardoya, R. (2008) *Mol. Biol. Evol.* **25,** 1043–1053
18. Frasca, F., Pandini, G., Scalia, P., Sciacca, L., Mineo, R., Costantino, A., Goldfine, I. D., Belfiore, A., and Vigneri, R. (1999) *Mol. Cell. Biol.* **19,** 3278–3288
19. Seino, S., and Bell, G. I. (1989) *Biochem. Biophys. Res. Commun.* **159,** 312–316
20. Mosthaf, L., Grako, K., Dull, T. J., Coussens, L., Ullrich, A., and McClain, D. A. (1990) *EMBO J.* **9,** 2409–2413
21. Moller, D. E., Yokota, A., Caro, J. F., and Flier, J. S. (1989) *Mol. Endocrinol.* **3,** 1263–1269
22. Navarrete Santos, A., Ramin, N., Tonack, S., and Fischer, B. (2008) *Endocrinology* **149,** 515–524
23. Louvi, A., Accili, D., and Efstratiadis, A. (1997) *Dev. Biol.* **189,** 33–48
24. Savkur, R. S., Philips, A. V., and Cooper, T. A. (2001) *Nat. Genet.* **29,** 40–47
25. Kellerer, M., Sesti, G., Seffer, E., Obermaier-Kusser, B., Pongratz, D. E., Mosthaf, L., and Häring, H. U. (1993) *Diabetologia* **36,** 628–632
26. Kosaki, A., and Webster, N. J. (1993) *J. Biol. Chem.* **268,** 21990–21996
27. Mosthaf, L., Vogt, B., Häring, H. U., and Ullrich, A. (1991) *Proc. Natl. Acad. Sci. U.S.A.* **88,** 4728–4730
28. Norgren, S., Zierath, J., Galuska, D., Wallberg-Henriksson, H., and Luthman, H. (1993) *Diabetes* **42,** 675–681
29. Norgren, S., Li, L. S., and Luthman, H. (1994) *Biochem. Biophys. Res. Commun.* **199,** 277–284
30. Brook, J. D., McCurrach, M. E., Harley, H. G., Buckler, A. J., Church, D., Aburatani, H., Hunter, K., Stanton, V. P., Thirion, J. P., Hudson, T., *et al.* (1992) *Cell* **69,** 385
31. Mahadevan, M. S., Yadava, R. S., Yu, Q., Balijepalli, S., Frenzel-McCardell, C. D., Bourne, T. D., and Phillips, L. H. (2006) *Nat. Genet.* **38,** 1066–1070
32. Ladd, A. N., Charlet, N., and Cooper, T. A. (2001) *Mol. Cell. Biol.* **21,** 1285–1296
33. Philips, A. V., Timchenko, L. T., and Cooper, T. A. (1998) *Science* **280,** 737–741
34. Liquori, C. L., Ricker, K., Moseley, M. L., Jacobsen, J. F., Kress, W., Naylor, S. L., Day, J. W., and Ranum, L. P. (2001) *Science* **293,** 864–867
35. Mankodi, A., Takahashi, M. P., Jiang, H., Beck, C. L., Bowers, W. J., Moxley, R. T., Cannon, S. C., and Thornton, C. A. (2002) *Mol. Cell* **10,** 35–44
36. Charlet-B, N., Savkur, R. S., Singh, G., Philips, A. V., Grice, E. A., and Cooper, T. A. (2002) *Mol. Cell* **10,** 45–53
37. Kosaki, A., Nelson, J., and Webster, N. J. (1998) *J. Biol. Chem.* **273,** 10331–10337
38. Sen, S., Talukdar, I., and Webster, N. J. (2009) *Mol. Cell. Biol.* **29,** 871–880
39. Caputi, M., Mayeda, A., Krainer, A. R., and Zahler, A. M. (1999) *EMBO J.* **18,** 4060–4067
40. Keene, J. D., Komisarow, J. M., and Friedersdorf, M. B. (2006) *Nat. Protoc.* **1,** 302–307
41. Tenenbaum, S. A., Lager, P. J., Carson, C. C., and Keene, J. D. (2002) *Methods* **26,** 191–198
42. Webster, N. J., and Huang, Z. (1999) *Front. Horm. Res.* **25,** 1–17
43. Vidal, H., Auboeuf, D., Beylot, M., and Riou, J. P. (1995) *Diabetes* **44,** 1196–1201
44. Warf, M. B., and Berglund, J. A. (2007) *RNA* **13,** 2238–2251
45. Ho, T. H., Charlet-B, N., Poulos, M. G., Singh, G., Swanson, M. S., and Cooper, T. A. (2004) *EMBO J.* **23,** 3103–3112
46. Hino, S., Kondo, S., Sekiya, H., Saito, A., Kanemoto, S., Murakami, T., Chihara, K., Aoki, Y., Nakamori, M., Takahashi, M. P., and Imaizumi, K. (2007) *Hum. Mol. Genet.* **16,** 2834–2843
47. Yuan, Y., Compton, S. A., Sobczak, K., Stenberg, M. G., Thornton, C. A., Griffith, J. D., and Swanson, M. S. (2007) *Nucleic Acids Res.* **35,** 5474–5486
48. Goers, E. S., Purcell, J., Voelker, R. B., Gates, D. P., and Berglund, J. A. (2010) *Nucleic Acids Res.* **38,** 2467–2484

49. Paul, S., Dansithong, W., Kim, D., Rossi, J., Webster, N. J., Comai, L., and Reddy, S. (2006) *EMBO J.* **25,** 4271–4283

50. Dansithong, W., Paul, S., Comai, L., and Reddy, S. (2005) *J. Biol. Chem.* **280,** 5773–5780

51. Savkur, R. S., Philips, A. V., Cooper, T. A., Dalton, J. C., Moseley, M. L., Ranum, L. P., and Day, J. W. (2004) *Am. J. Hum. Genet.* **74,** 1309–1313

52. Warf, M. B., Nakamori, M., Matthys, C. M., Thornton, C. A., and Berglund, J. A. (2009) *Proc. Natl. Acad. Sci. U.S.A.* **106,** 18551–18556

53. Kanadia, R. N., Shin, J., Yuan, Y., Beattie, S. G., Wheeler, T. M., Thornton, C. A., and Swanson, M. S. (2006) *Proc. Natl. Acad. Sci. U.S.A.* **103,** 11748–11753

54. Licatalosi, D. D., Mele, A., Fak, J. J., Ule, J., Kayikci, M., Chi, S. W., Clark, T. A., Schweitzer, A. C., Blume, J. E., Wang, X., Darnell, J. C., and Darnell, R. B. (2008) *Nature* **456,** 464–469

55. Warf, M. B., Diegel, J. V., von Hippel, P. H., and Berglund, J. A. (2009) *Proc. Natl. Acad. Sci. U.S.A.* **106,** 9203–9208

56. Castle, J. C., Zhang, C., Shah, J. K., Kulkarni, A. V., Kalsotra, A., Cooper, T. A., and Johnson, J. M. (2008) *Nat. Genet.* **40,** 1416–1425